IMAGE CORRELATION ANALYSIS OF MULTIPLE-BOLT WOOD CONNECTIONS

John W. Stelmokas
Chemist, Technical Development
Kanzaki Speciality Papers
22 Cummings St, Ware, MA 01082-2002

Audrey G. Zink
Assistant Professor

and

Joseph R. Loferski
Associate Professor
Wood Science and Forest Products
Virginia Tech, Blacksburg, VA 24062-0323

(Received November 1996)

ABSTRACT

Displacement beneath the bolts in multiple-bolted wood connections was studied using digital image correlation. This method combines digital image analysis and image correlation to calculate surface displacements from a set of digitized video images of an object under an applied load. Double-shear connections constructed of clear, straight-grained yellow-poplar were tested in compression parallel to grain. Five different bolt patterns were used to analyze the effect of number of bolts in a vertical row and number of bolts in a horizontal column on displacement distribution among bolts. It was discovered that for multi-bolt patterns in a vertical row, parallel to load displacements below the outer bolts, are higher than those below the center bolt(s) but not equal in magnitude as previously assumed and the surface displacements perpendicular to the load beneath the bolts split along the centerline of the bolts. Variation in material properties, rigid body motion, eccentric loading and/or wood failure beneath a bolt are detectable with digital image correlation and may influence the results if not carefully considered in experimental design.

Keywords: Multiple-bolted wood connections, digital image correlation, displacement analysis, mechanical connections, double shear joints.

INTRODUCTION

It is well documented that the connections in structures are the most critical component in ensuring structural integrity and performance. In concrete and steel structures, the behavior has been well researched. However, in wood structures the behavior of the connections has been difficult to determine. Our knowledge of connection behavior is insufficient primarily in the area of multiple-bolted wood connections. The limiting factor has been the experimental techniques applicable for analyzing the connections.

The objective of this study was to investigate a new technique called the digital image correlation technique (DICT) to improve the understanding of bolt displacement in multiple-bolted wood connections. DICT combines digital image analysis and image correlation to calculate surface displacements from a set of digitized video images of an object under an

applied load. This method has been demonstrated to measure quickly and accurately full-field surface displacements in fields such as rigid body mechanics (Peters et al. 1983), fluid mechanics (He et al. 1984), experimental mechanics (Chu et al. 1985), biomechanics (Ranson et al. 1986), fracture mechanics (Luo et al. 1994), micromechanics (Vendroux 1994), and wood science (Agrawal 1989; Choi et al. 1991; Zink et al. 1995). However, it has yet to be applied to bolted wood connections. Because information regarding individual bolt behavior could be obtained from full-field displacement data of the wood surface around the bolts, it is proposed the DICT could be a suitable experimental technique to study multiple-bolted wood connections.

While this particular report on bolted wood connections is limited to the displacement patterns near the bolts, the load distribution and assessment of design procedures for these connections are available in two other reports by the authors (Stelmokas et al. 1997 and Salenikovich et al. 1996, respectively).

BACKGROUND

Several experimental techniques have been utilized to study the associated stresses and strains in the neighborhood of a loaded bolt hole. Information gained from these techniques has occasionally been used to analyze multiple-bolted connection behavior. Strain gages and moiré interferometry have been the traditional techniques used. These two methods have been primarily employed to experimentally verify analytical models developed by researchers (Wilkinson and Rowlands 1981; Rowlands et al. 1982; Rahman et al. 1991). In order to measure the load distribution among a row of bolts, Wilkinson (1986) developed a variation of traditional strain gages. Load cells were constructed by bonding strain gages between each set of holes on the steel side plates of the connection. "The gages were connected to provide a single output for each hole" from which the load carried by each bolt in the row could be computed (Wilkinson 1986). In general, strain gages have a very limited gage length and may not detect critical areas of the strain distribution, especially with wood specimens. Moiré interferometry operates on the principle of interference by determining the difference in movement between an undeformed reference grating and a deformed object grating. Because of the complexity of its application, moiré interferometry has not received widespread use in wood engineering studies.

Humphrey and Ostman (1989 a, b) have developed two techniques, one to model wood deformation around bolts and the other to study bending and overall displacement of bolts within connections. As reported in Part I of their study, a steel pin is passed through thin wood wafers that are between glass plates. These wafers are stressed in tension, and the associated wood deformation and failure around the pin are photographed. Multiple pin wafers were also tested. In Part II of their study, X-ray scans were used to observe and quantify the bending and overall displacement of a single bolt within a joint as the joint is loaded in tension to failure. When the X-ray data were used in conjunction with load-slip data, the associated wood deformation within the joint could also be determined. It was further suggested that when this X-ray technique is combined with the wafer technique, connection performance (both wood and entire bolt behavior) throughout the joint can be evaluated.

The technique developed by Humphrey and Ostman (1989a) was used by Fantozzi and Humphrey (1995) to analyze the effects of bending moments on multiple-bolted wood connection behavior. Results suggest that the technique may be useful for developing joint designs and looking at the effects of wood variables. However, this technique has yet to be applied to full-size connections and thus may be impractical to use.

An optical technique has been developed by Kermani and McKenzie (1994) to study strain distributions around a single bolt. Kermani and McKenzie used single-beam reflection ho-

lography to study the effects of grain angle on the behavior of a single-bolted connection in compression. The researchers obtained results for both in-plane and out-of-plane displacements with this technique and showed that the strain distributions around the bolt were highly dependent on the grain orientation of the specimen. This technique can be difficult, expensive, and has yet to be applied to multiple-bolted connections.

In the field of wood and wood products, various experimental techniques have been used to quantify surface deformations and thus provide strain information on wood specimens under load. While many of these methods may provide accurate results, certain limitations are associated with each technique. Previously, dial gages, electrical strain gages, and linear variable differential transformers (LVDTs) have been the conventional devices utilized to measure point-source displacements in wood specimens. The limitation of these methods is that they can only measure displacements over a very limited gage length and thus cannot be used to measure displacements (strains) over the entire surface of a specimen i.e. full-field deformations. Brittle coatings, laser speckle interferometry, moiré interferometry, photoelasticity, and single-beam reflection holography are some of the other methods that have been employed to measure strain in wood, especially with respect to full-field strain measurement.

The digital image correlation technique (DICT) is a relatively new method in experimental mechanics that can be used for full-field deformation measurements. DICT combines digital image analysis and image correlation to calculate surface displacements from a set of digitized video images of an object under an applied load. Choi et al. (1991) explained that the fundamental concept of the DICT is that a "digital computer recognizes a light intensity pattern of a small area in an undeformed image and then finds the same area in a deformed image." Typically, two or more video images are acquired with a charged coupled device (CCD) video camera, "one of which [is] undeformed and the others of which [are] deformed" (Choi et al. 1991), of an object surface that has a varying light intensity pattern. The images are digitized (i.e. each intensity value is assigned a binary number that corresponds to a gray level) and stored in computer memory or on disk for future reference. Each image is now a measured intensity pattern and "represents the positions of points on the surface of" an object (Sutton and Chao 1988).

Small subsets of the undeformed and deformed images are chosen. A computer program mathematically cross-correlates the chosen subsets by comparing the subset "from the undeformed image to subsets from each of the other [deformed] images until the best match is obtained. The difference in the location of the subset before and after deformation is the displacement" (Sutton and Chao 1988). By choosing different subsets, the displacement of numerous points on the surface of the object can be calculated. The mathematical techniques necessary for cross-correlating the undeformed, reference image with a deformed image were developed by Peters and Ranson (1982).

DICT has recently been applied to wood and wood products with the results indicating that it is a viable method for studying complex wood behavior. Agrawal (1989) used digital image processing to study the full-field deformations of wood and aluminum specimens loaded in compression and bending and to monitor the creep response of wood. Choi et al. (1991) used DICT to measure displacement and strain in very small specimens of wood and paper. Their results were compared to a photographic method and showed good agreement. Zink (1992) used the technique to experimentally determine the influence of overlap length on the strain distribution and the progressive failure behavior of a bonded wood double lap joint.

MATERIALS AND METHODS

Specimen description

Test specimens were three-member, double-shear connections loaded parallel to the grain.

This configuration was selected to reduce eccentricity problems associated with two-member connections and so that the side member surface could be visible for imaging purposes. Yellow-poplar (*Liriodendron tulipfera*) was used because its uniform, diffuse-porous anatomy would minimize the effects of the earlywood/latewood differences and material inhomogeneity on surface deformations. Prior to machining, the lumber was conditioned in an environmental chamber for approximately two months where the temperature and humidity were controlled to correspond to an approximate moisture content of 12% per ASTM D 1761 (ASTM 1993) specifications for testing mechanical fasteners.

The effect of bolt configuration on the distribution of displacement among the bolts was determined using the following variables: number of bolts in a vertical row (1,2,3) and number of bolts in a horizontal column (1,2,3). These joint variables were selected to confirm and/or expand the knowledge of multiple-bolted connection behavior based on the needs identified in the literature. Five different bolt patterns were used as illustrated in Fig. 1: pattern #1 is a single bolt; pattern #2 is a vertical row of two bolts; pattern #3 is a vertical row of three bolts; pattern #4 is a horizontal column of two bolts; and pattern #5 is a horizontal column of three bolts. Three replications of each bolt pattern were tested. The National Design Specifications (AFPA 1993) recommended spacing between bolts in a row (4D—4 times the bolt diameter D) and edge (1.5D) and end (4D and 7D) distances for full design value were met or exceeded for all specimens. The bolt holes were drilled 0.07 mm (1/32 inch) oversize for bolt tolerance.

Digital image correlation

Digital image correlation requires capturing video images of a properly illuminated specimen as it is being loaded, digitizing these images, and mathematically cross-correlating the reference and deformed images to calculate displacements. A Panasonic WV-CL350 Color CCTV charged-coupled device (CCD) video camera, high resolution Panasonic CT1383Y color video monitor, 70-mm Nikon zoom lens, and a SUN SPARC10 Model 40 workstation computer with digitizing board were used to acquire and digitize the video images. A standard C-mount adapter was used to attach the zoom lens to the video camera. The video camera was mounted on a Bogen 3021 professional tripod. Two white light 150W photoflood lights with aluminum shields were used to illuminate the specimens during testing. These lights were mounted on each side of the video camera. A level, ruler, and tape measure were used to align the specimens with the video camera. The Fortran program used for the mathematical cross-correlation uses a coarse-fine searching method to locate subsets before and after deformation, minimization of a cross-correlation coefficient to establish the best-fit of the subsets, and a bilinear interpolation scheme to interpolate gray levels between pixel locations. The procedure is fully described by Zink et al. (1995).

Several preliminary experiments were conducted to evaluate the digital image correlation system (camera, lens, illumination source, hardware, and software). Evaluation tests included determining the baseline noise of the system, the effect of out-of-plane motion, and the accuracy in measuring two-dimensional (in-plane) rigid body motion. Evaluations were conducted using a 2.54 × 2.54 × 8.57 cm (1 × 3.375 inch) aluminum block with an extension rod mounted in a Boeckeler Instruments #12625 extensometer calibrator. The extensometer is a device that is capable of accurately moving an object distances measurable to 0.00254 mm (0.0001 inch), and it is often used to calibrate LVDTs. The evaluation procedures and results are fully described in Stelmokas (1995). In summary, it was found that baseline noise levels were acceptably small and would not interfere with displacement measurements, no distortion of the results would be introduced from out-of-plane motion of the test specimens, and the rigid body motion measured with the correlation

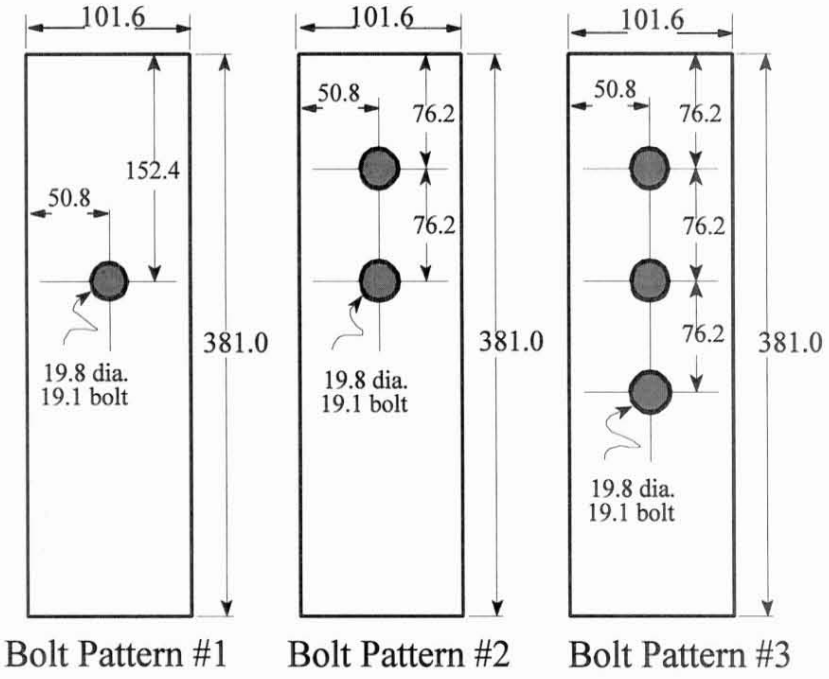

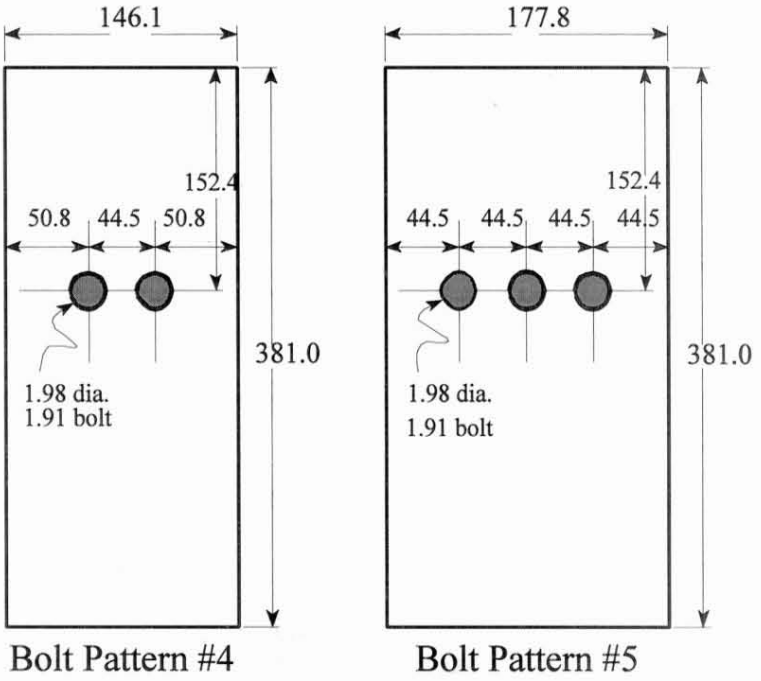

FIG. 1. Diagram and dimensions (mm) of the 5 bolt patterns tested.

FIG. 2. Photograph displaying the aluminum block evaluation test setup.

technique matched very well with the extensometer displacement motion with a 4.52% error in the horizontal motion and a 6.5% error in the vertical motion measurements.

Variability in the measurements that might be expected from material inhomogeneity was tested in two more preliminary compression tests. The first test used an aluminum block, and the second used seven blocks of yellow-poplar wood from the joint specimen test material. Aluminum was chosen because it is considered an isotropic, homogeneous material with known mechanical properties. The aluminum block was 166 mm (6.542 inch) parallel to the load and 102 mm × 38.8 mm (4.016 in × 1.530 inch) in cross section. The wood blocks averaged 205 mm (8.063 inch) parallel to the load and 100 mm × 48.26 mm (3.960 inch × 1.900 inch) in cross section. A spherical ball and socket bearing seat were used at the bottom of the specimen to minimize eccentric loading. A steel block was used at the top of the specimen to distribute the applied compression load over the entire specimen cross section. Compression tests were conducted only within the linear elastic range as determined by the shape of the load/deflection curves. The mechanical test setup is illustrated in Fig. 2. DICT was used to measure the in-plane displacements of 20 points on the surface of the aluminum test specimen using a matrix of 4 rows and 5 columns. Displacement evaluation procedures are fully described by Stelmokas (1995). In summary, the average in-plane displacements for the aluminum and wood blocks are shown in Table 1 at a compression load of 180 kN (40,000 lb). Examination of Table 1 indicates that variability in a single horizontal line of data across the face of the test specimens is minimal for the aluminum compression block, and as might be expected, slightly higher in the wood block. Because the load was applied to the end of the test specimens nearest row #1, the displacements reported in Table 1 are highest nearest the loaded end and decrease uniformly away from the load. These preliminary evaluation tests indicate that the level of variability expected from just material heterogeneity, such as might be expected with a diffuse porous wood specimen, is quite small.

TABLE 1. *Displacement measurements (in units of mm) using a matrix of 4 rows and 5 columns for wood and aluminum compression tests. Load = 180 kN (40,000 lbs).*

	Wood					Aluminum				
	Column					Column				
Row	1	2	3	4	5	1	2	3	4	5
1	0.498	0.531	0.498	0.494	0.491	0.085	0.105	0.105	0.108	0.103
2	0.458	0.464	0.444	0.404	0.424	0.080	0.085	0.082	0.090	0.095
3	0.411	0.414	0.360	0.374	0.371	0.065	0.063	0.070	0.082	0.090
4	0.371	0.381	0.284	0.251	0.237	0.068	0.065	0.060	0.063	0.073

For mechanical testing of the bolted joint testing, the test assemblies were positioned in the testing machine and the load applied; digital images were acquired at several load levels within the elastic range of load/displacement behavior based on visual examination of the real-time load/displacement plot from the testing machine. The reference image for all bolt patterns was acquired at 2.224 kN (500 lb). This load level was chosen to allow the bolted connections to align so that any rigid body motion associated with the alignment would be minimized. For bolt pattern #1, subsequent deformed images were acquired at 2.224 kN (500 lb) increments and at 4.448 kN (1000 lb) increments for all other bolt patterns (2–5). Three load levels—low, medium, and high—were chosen as the deformed images for later analysis. Images were acquired until visible wood failure was observed and the rate of loading slowed considerably as determined by the testing machine display and nonlinear load vs. time curve viewed during data acquisition.

Measurement grids of 7×9 points for bolt patterns #1, #2, and #3 and 11×9 points for bolt patterns #4 and #5 were chosen to study the surface displacements beneath the bolt(s). The location of each data point on the surface of each bolt pattern is shown in Fig. 3, where the black crosses indicate the data point locations. Displacements were obtained both parallel (vertical direction) and perpendicular (horizontal direction) to the applied load.

Testing machine

A servo-hydraulic Material Test System (MTS) testing machine was used to apply load to all specimens in this research. A ±220 kN (50,000 lb) load cell, a ±90 kN (20,000 lb) load range card, and a ±15.24-mm (0.600 inch) deflection range card were used to control and monitor tests. Connections were loaded at a deflection-controlled rate of 0.508 mm (0.020 inch) per minute according to ASTM D 1761 (ASTM 1993) specifications. To position the specimens inside the MTS so that they were in the center of the hydraulic ram and parallel with the camera, angle-iron braces were fastened to the MTS table at the bottom of each side member. The angle-iron braces also prevented the side members from moving outwards during testing. A wood block placed between the side members at the bottom of the connection prevented members from moving inwards. A small elastic band was stretched around the top of the single-bolted connections to keep the members in alignment.

A spherical ball and socket bearing seat were mounted on the load cell of the MTS to help minimize eccentric loading. Two steel blocks with a total thickness of 63.5 mm (2.5 inch) covering the entire cross-sectional area of the main member were inserted between the bearing seat and the top of the specimen to distribute the applied load evenly. A steel plate was placed between the bottom of the connection and the testing machine table to give the specimen a smooth, flat bearing surface. Figure 4 illustrates the joint test setup and apparatus used to ensure uniform loading.

RESULTS AND DISCUSSION

The digital image correlation results are presented as contour plots of the in-plane displacement fields for both parallel (y-direction) and perpendicular (x-direction) to load at three selected load levels. In-plane displacements were obtained for each data point illustrated in Fig. 3. Due to the origin of computerized digital images being in the upper left-hand corner, for perpendicular to load (x) displacements, motion to the left is considered negative and motion to the right is considered positive; and for parallel to load (y) displacements, up is negative and down is positive. The x and y coordinates of the contour plots correspond exactly to the dimensions imaged on each side member using the upper left-hand corner of the member as the origin, i.e., point (0,0). The rectangular area within the x and y coordinates where the contours are plotted corresponds to the placement of the measurement grid on the specimen surface. Displace-

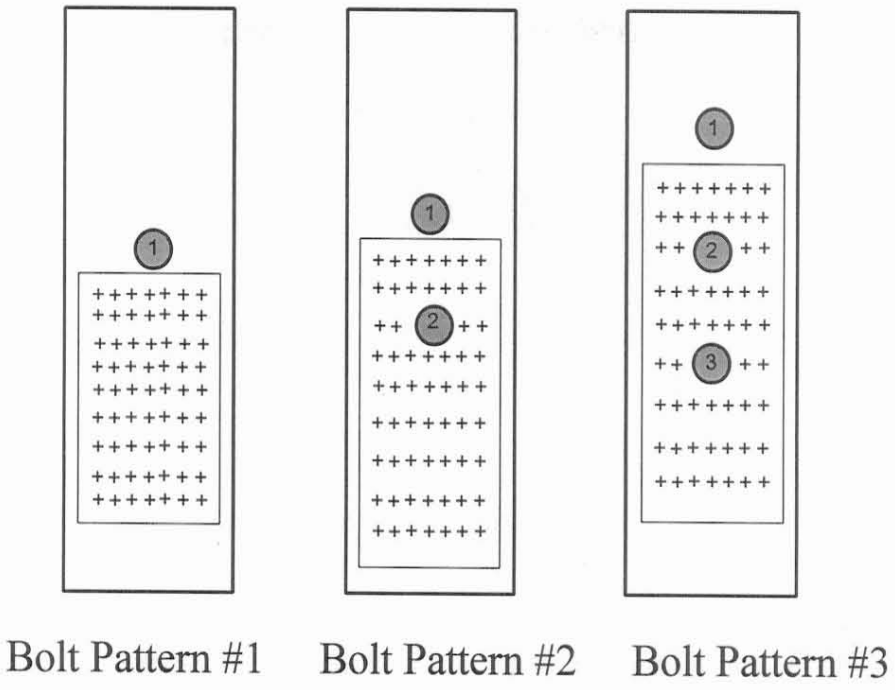

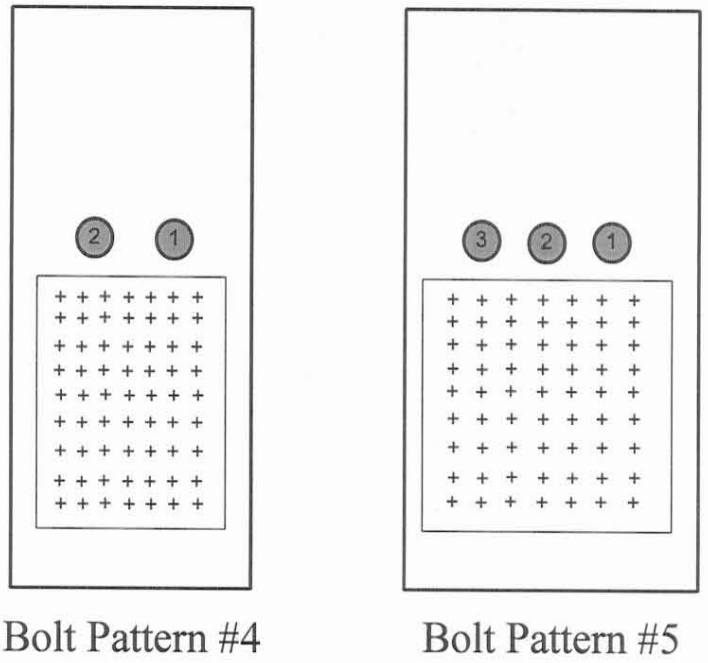

FIG. 3. Diagram of measurement point locations on test specimen surfaces. The black crosses indicate data point locations, the numbers on the circles indicate bolt number.

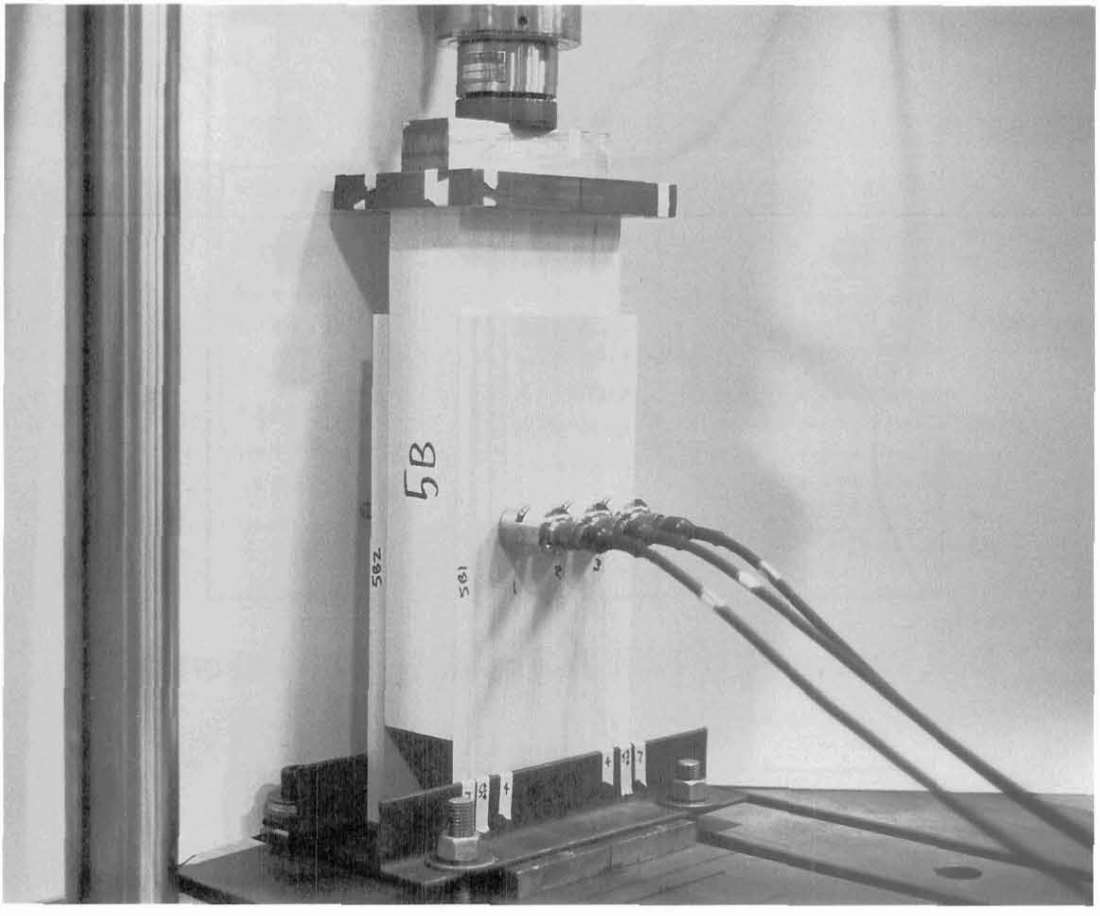

FIG. 4. Photograph of a three-member wood connection showing testing machine, loading setup, and test specimen configuration.

ment results are in units of microns (mm $\times$ 10^{-3}). The solid black circles in these figures represent the location and size of the bolts on the specimen surface relative to the measurement grid, and the white numbers are to identify each bolt. Bolts move downward parallel to load as the load increases; thus wood surface displacements occur primarily beneath the bolt. Load levels refer to the load at which the images were acquired.

Perpendicular to load displacement results of bolt pattern #1—a single bolt—are displayed in Figs. 5A–5C for specimen B. Because the single bolt was in the middle of the measurement grid and moving downwards, displacements left (negative) and right (positive) were expected due to the Poisson effect of lateral expansion perpendicular to the applied compression force of the bolts. However, none of the single bolt connections displayed this trend. Specimen B (shown in Figs. 5A–5C) shows all displacements as moving right as the load increases. These results suggest eccentric loading of the connection and/or main member rotation about the single bolt, which may cause rigid body motion. Figures 5D–F display the parallel to load displacement results for specimen B, bolt pattern #1. It is seen in these figures that as the load increases, displacements steadily increase downward (positive), and the highest displacements appear to be concentrated beneath the bolt. This trend was also observed for the other

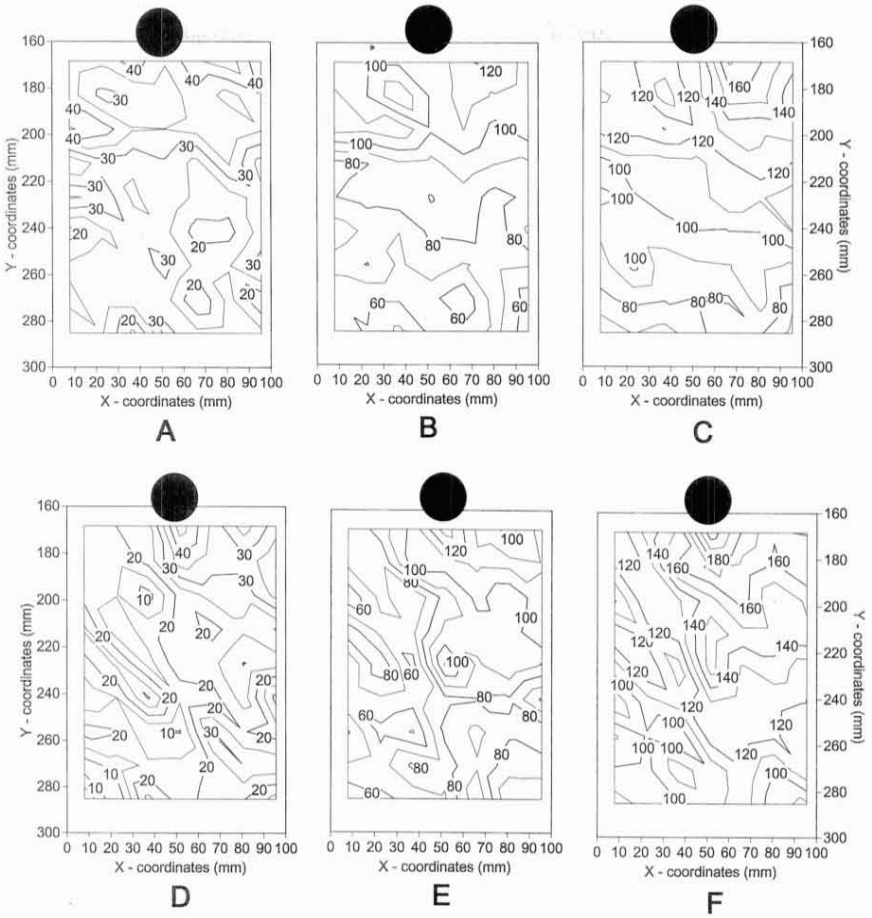

FIG. 5. Contour plots of the displacement fields for bolt pattern #1; Displacements in mm × 10^{-3} (0.03937 in × 10^{-3}); A–C: perpendicular to load; D–F: parallel to load; A. & D. load = 4.448 kN (1,000 lb), B. & E. load = 11.12 kN (2,500 lb), C. & F. load = 17.792 kN (4,000 lb).

single bolt connections and was expected due to the downward motion of the bolt.

Perpendicular to load displacement results of bolt pattern #2—vertical row of two bolts—are shown in Figs. 6A–6C for a representative specimen (A). At 2.224 kN (5000 lb), it appears that all displacements are moving right. But at 4.003 kN (9000 lb), movement left and right appears to be happening where the graph is separating into two halves along the line of the bolts. It is possible that early in the test, rigid body motion or eccentric loading occurred. But later in the test, the connection may have aligned itself, and the motion of the bolts caused displacements left and right to take place. Specimen B (not shown) displayed the same trend as specimen A. However, specimen C (not shown) displayed results similar to those observed for specimen 1B (Figs. 6A–6C) where all perpendicular displacements appeared to move right. It is unknown why the perpendicular results of specimen C differed from specimens A and B except for possible rigid body motion of the entire connection, eccentric loading, or wood failure beneath the bolts.

Parallel to load displacements of specimen 2A are shown in Figs. 6D–F. The progressive load series clearly displays the creation of the displacement fields and how the highest displacements on the surface are concentrated beneath each bolt. The shapes of these

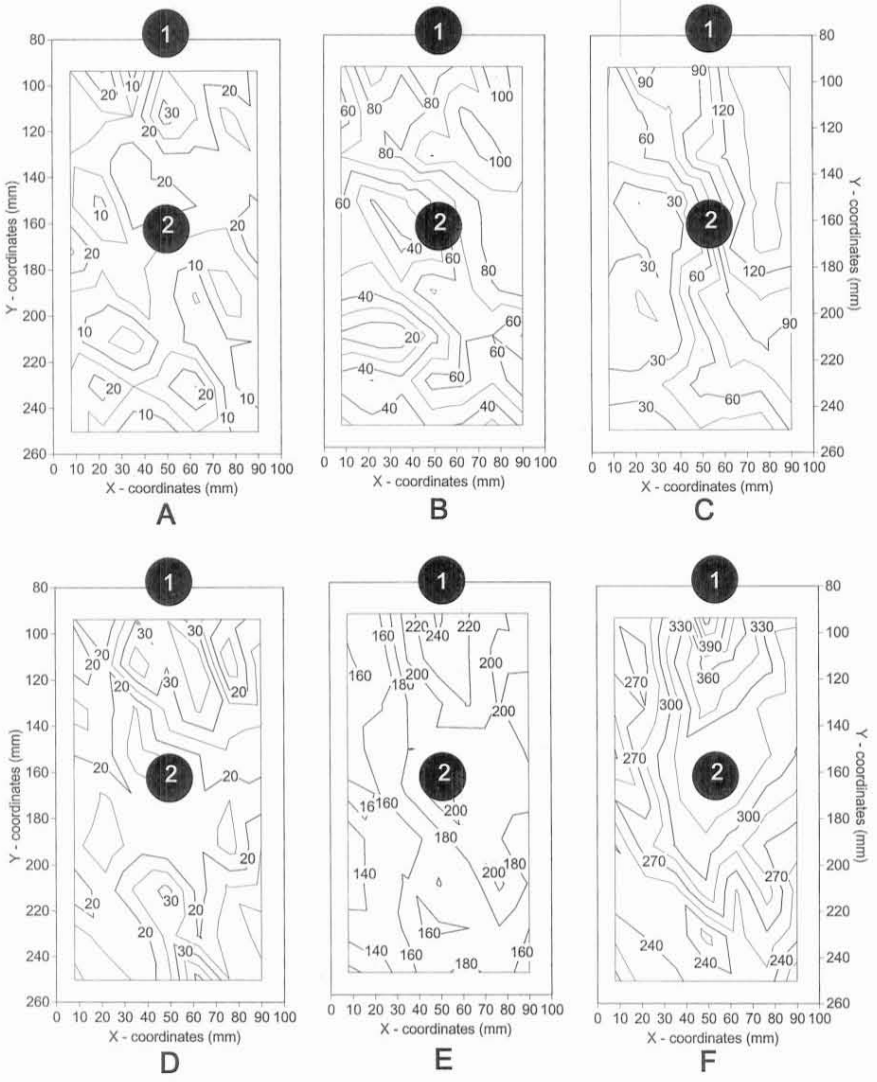

FIG. 6. Contour plots of the displacement fields for bolt pattern #2; Displacements in mm × 10^{-3} (0.03937 in × 10^{-3}); A–C: perpendicular to load: D–F: parallel to load; A. & D. load = 4.448 kN (1,000 lb), B. & E. load = 22.24 kN (5,000 lb), C. & F. load = 40.03 kN (9,000 lb).

fields are very similar to those observed for bolt pattern #1. However, displacements below the top bolt (#1) were slightly higher than those beneath the bottom bolt. This trend was also observed for specimens B and C (not shown) of pattern #2. If a uniform strain is assumed to exist across the cross section of the member, the higher displacements below the top bolt than those below the bottom bolt can be explained by the different distances between the bearing area below each bolt and the fixed bearing area at the bottom of the connection. The bearing area below the top bolt has a longer distance to the fixed end than the bearing area below the bottom bolt. Because deformation is a cumulative response, a longer distance between the bearing area below a bolt and the fixed end of the side member will correspond to higher displacement below that bolt. Therefore, the observed trend of higher displacements below the top bolt can be ex-

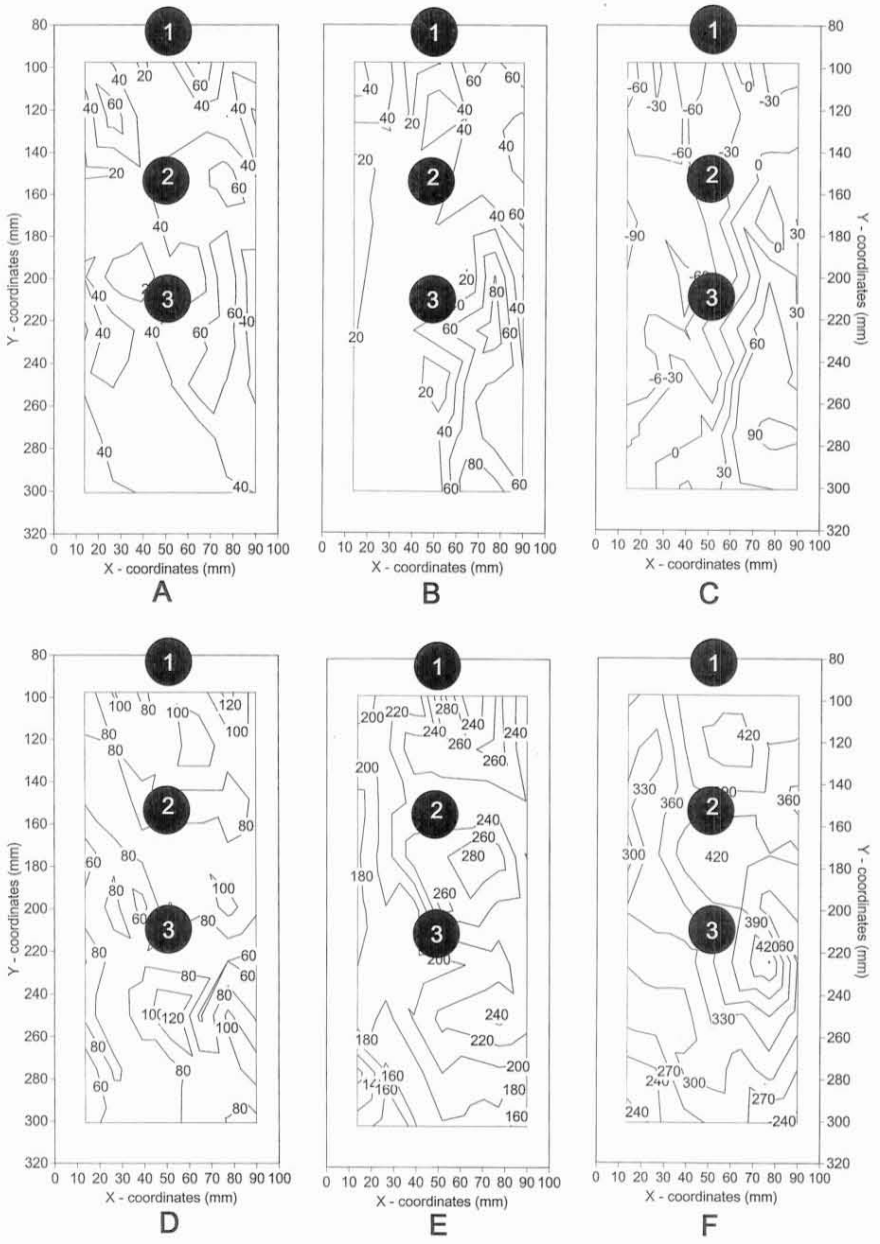

FIG. 7. Contour plots of the displacement fields for bolt pattern #3; Displacements in mm × 10^{-3} (0.03937 in × 10^{-3}); A–C: perpendicular to load; D–F: parallel to load; A. & D. load = 8.896 kN (2,000 lb), B. & E. load = 35.58 kN (8,000 lb), C. & F. load = 62.27 kN (14,000 lb).

plained by its longer distance to the fixed end of the member relative to the bottom bolt.

Figures 7A–C display perpendicular to load displacement results for representative specimen C of bolt pattern #3—vertical row of three bolts. Early in the test (load levels 8.896 kN and 35.584 kN (2,000 and 8,000 lbs) it appears that there is rightward movement on the surface. However, at load level 62.272 kN (14,000 lbs), the left half of the member is moving left and the right half is moving right

with almost zero displacements along the line of the bolts. This trend suggests that the downward motion of the bolts as the load is increased causes the connection to split apart along the line of the bolts. This is most likely due to the Poisson ratio effect causing lateral expansion perpendicular to the applied compression force of the bolts and low tension perpendicular strength. However, specimen B (not shown) displayed results similar to those observed for specimen 1B (Fig. 5A–5C), where all perpendicular displacements appeared to move right. The results of specimen B differed from specimens A and C probably due to rigid body motion of the entire connection and/or eccentric loading.

The parallel to load displacements of bolt pattern #3 are shown in Figs. 7D–7F for specimen 3C. Once again, the highest displacements on the surface are concentrated beneath the bolts, especially at the highest load. The shapes of the displacement fields are very similar to those observed for bolt patterns #1 and #2. However, displacements on the right side of the connection appear to be higher than the left side for each specimen. Furthermore, there appears to be an area of high displacements directly to the right of bolt #3 in specimen C. This trend was also observed, although not as pronounced, in specimen B (not shown). Upon inspection of specimens B and C, there were no visible surface defects to explain this high concentration of displacements. It is possible that the natural variability of wood caused these high displacements. Also, the displacements parallel to load below the top bolt were higher than those below the bottom two bolts for all specimens. As described for bolt pattern #2, this can be explained by the longer distance of the top bolt to the fixed bearing end of the side member relative to the bottom two bolts. Because deformation is a cumulative response, a longer distance will correspond to higher displacements.

Based on the perpendicular to load results of Figs. 5, 6, and 7, it appears that as the number of bolts in a vertical row increases, the "split" down the middle becomes more pronounced where the left half of the connection moves left and the right half of the connection moves right. This occurs because of the higher total applied load to the connection and because there are more bolts moving downwards in one line, thus increasing the tendency of the connection to "split" due to the Poisson effect of lateral expansion perpendicular to the applied compression force of the bolts and low tension perpendicular to the grain properties. If the load on the joints had been allowed to continue until failure, the displacements perpendicular to the grain caused by the wedge effect of the fasteners would lead to splitting of the side members. This splitting behavior of wood members parallel to a vertical row of fasteners has been observed often in practice and is reported to be the cause for connection failure at lower than expected loads (Jorissen 1996). Jorissen (1996) further indicates that in his study "the load carrying capacity of a multiple fastener connection is governed by crack developing at the loaded end instead of crack propagation near the hole." These findings agreed with the splitting of the displacement fields observed in this study illustrated in Figs 5, 6, and 7 and point out the ability of DICT measurements to predict the onset of splitting or cracking.

A clear-cut trend for the parallel to load displacements did not appear to develop between bolt patterns #1, #2, and #3. The parallel to load displacements did increase in magnitude as the number of bolts in a vertical row increased. For an equivalent load per bolt, higher displacements will occur parallel to load as the number of bolts in the connection increases. It is also possible that due to dissimilar side members, differences in material properties through the thickness of the wood members, and the fact that bolt loading is not unidirectional, the displacements may be greater on the inner side of the members or else the load is not symmetrically distributed between side members.

The perpendicular to load displacement results of bolt pattern #4—horizontal column of two bolts—are displayed in Figs. 8A–C for a

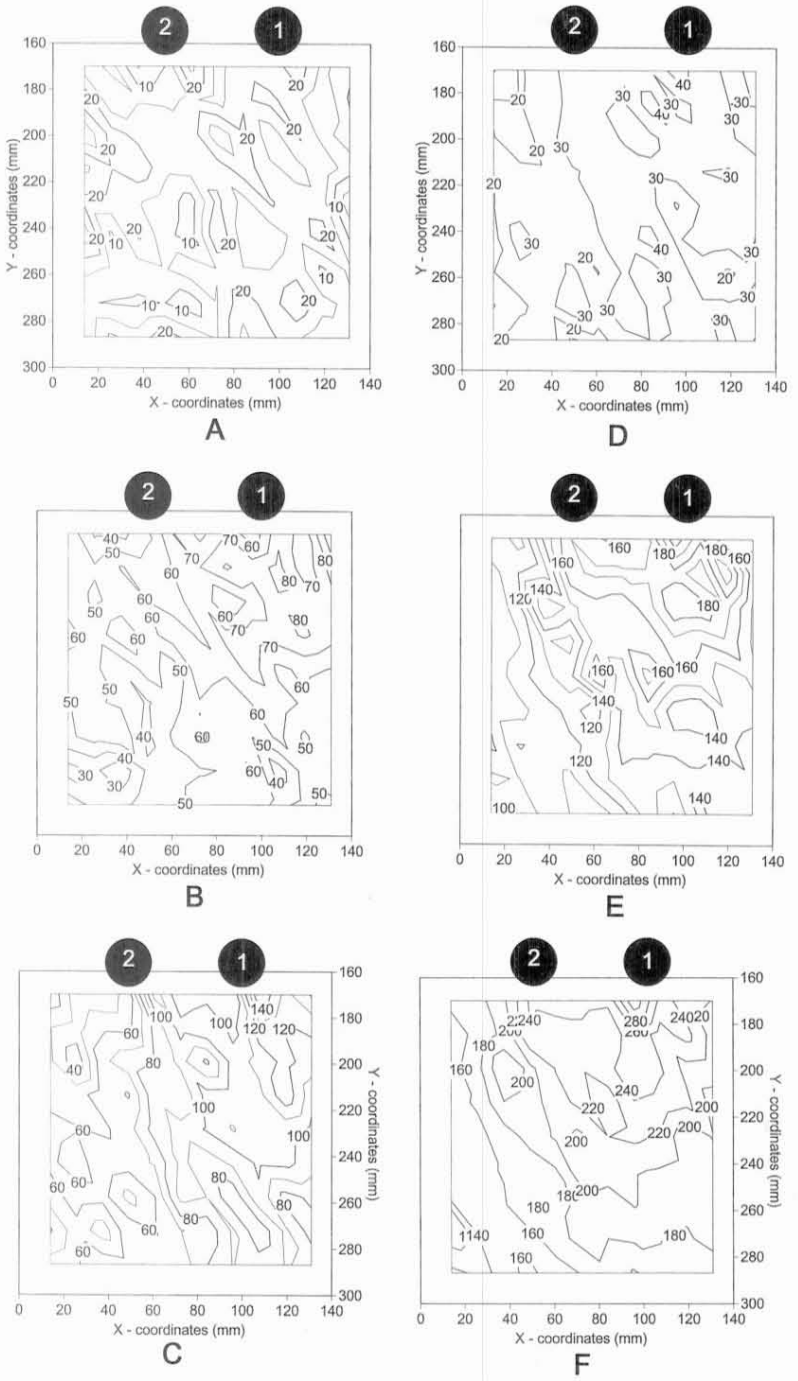

FIG. 8. Contour plots of the displacement fields for bolt pattern #4; Displacements in mm $\times 10^{-3}$ (0.03937 in $\times 10^{-3}$); A–C: perpendicular to load; D–F: parallel to load; A. & D. load = 4.448 kN (1,000 lb), B. & E. load = 17.79 kN (4,000 lb), C. & F. load = 26.69 kN (6,000 lb).

representative specimen (C). The increasing load series shows the development of the negative (leftward) displacement field to the left of bolt #2 and the positive (rightward) displacement field to the right of bolt #1 with zero displacements between the bolts. It is suggested that the downward motion of the bolts caused the surface beneath each bolt to move left and right, thus explaining the above observation. The zero displacements between the bolts were caused by the rightward motion below bolt #2 and the leftward motion below bolt #1 canceling each other out. This trend was also observed for specimen B (not shown). However, specimen A (not shown) displayed results similar to those observed for specimen 1B (Fig. 5) where all perpendicular displacements appeared to move right, indicating eccentric loading due to material character.

Figures 8D–F display the parallel to load displacement results of bolt pattern #4 for specimen C. Once again, the highest displacements on the surface are clearly concentrated below the bolts, especially at the highest load. In this specimen, C, the displacements were higher beneath bolt #2 than bolt #1. In specimen B (not shown) the displacements beneath each bolt were equal in magnitude. In specimen A (not shown) the displacements below bolt #1 are higher than those beneath bolt #2. Because the distances between the bearing area of each bolt and the fixed bearing end of the side member were equal, it is unknown why the parallel to load displacement observations differed for each specimen. It is probable that wood failure beneath the bolts or the inherent natural variability of wood caused the observed differences.

The perpendicular to load displacement results of bolt pattern #5—horizontal column of three bolts—are displayed in Figs. 9A–C for specimen A. In specimen A, all displacements appeared to be moving left, especially on the left half of the connection. There is slight movement right between load levels 2 and 3 to the right of bolt #1. However, in specimens B and C (not shown), all displacements appeared to be moving to the right. But there is also slight movement left between load levels 2 and 3 to the left of bolt #3. These are clearly equal and opposite trends, but it is unknown why they occurred. The downward motion of the bolts, rigid body motion of the entire connection, eccentric loading, and/or wood failure beneath the bolts are all factors that could explain these observations.

Figures 9D–F display the parallel to load displacement results of bolt pattern #5 for a representative specimen (A). The progressive load series clearly shows the development of the displacement fields with the highest surface displacements occurring directly beneath the bolts. The parallel to load displacements appear to be highest beneath the middle bolt (bolt #2) and approximately equal below the outer two bolts. This was also observed for specimens B and C. Because the distances between bearing area of each bolt and the fixed end of the side member were equal, the higher displacements below the middle bolt should occur due to the smaller tributary area beneath that bolt compared to the outer two bolts. A smaller tributary area causes a high stress and therefore a higher strain and displacement to occur below the middle bolt.

There did not appear to be any development of a well-defined trend in the surface displacements perpendicular to load as the number of bolts increased between bolt patterns #1, #4, and #5. The perpendicular displacements may or may not be concentrated on one side of the connection, which indicates less of a tendency of the wood side members to split perpendicular to the grain as the number of bolts increases in a horizontal column. However, the parallel to load displacements did increase in magnitude as the number of bolts in a horizontal column increased due to the increase in total applied load.

CONCLUSIONS

This research supports the following conclusions:

- As the number of bolts in a vertical row

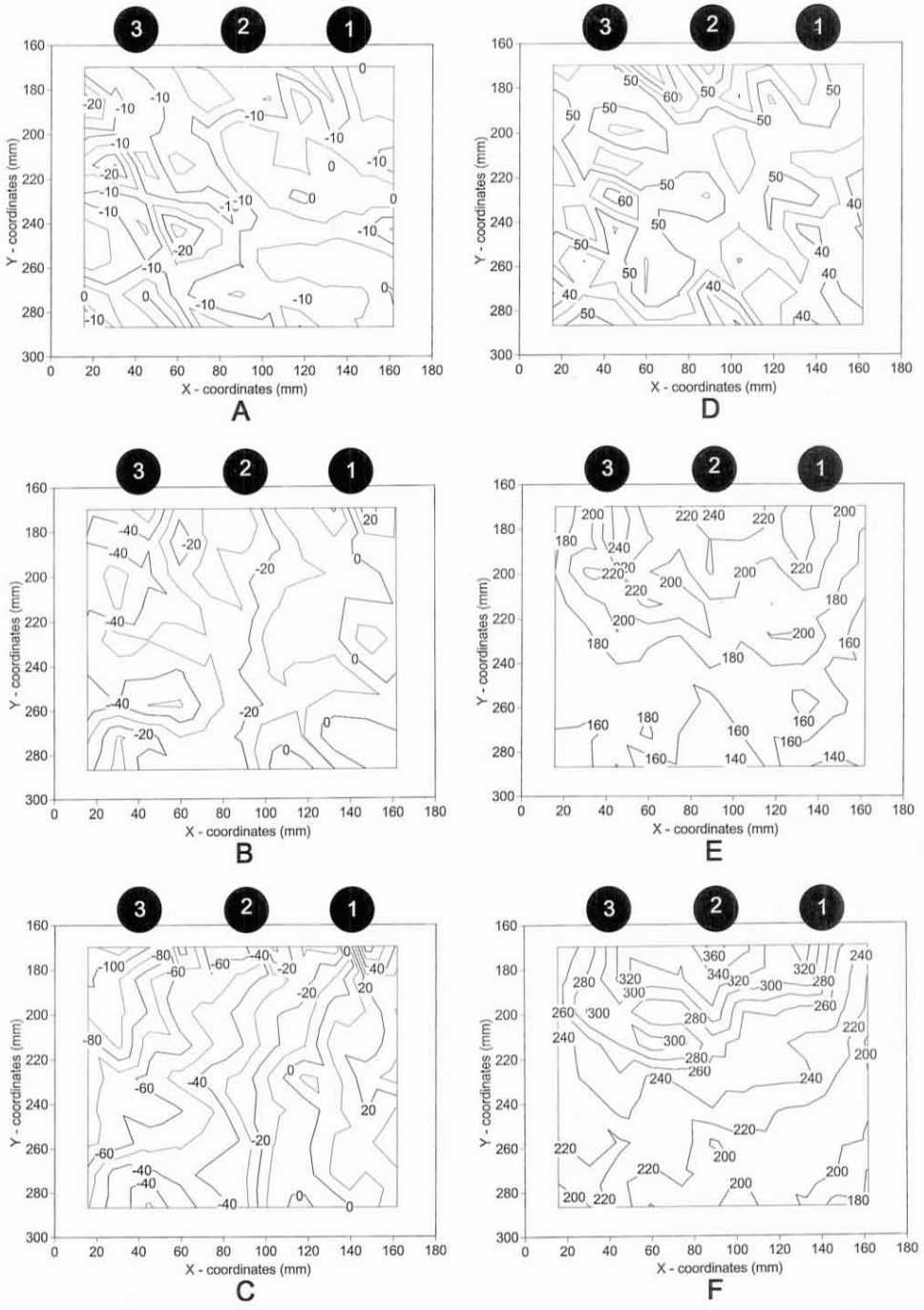

FIG. 9. Contour plots of the displacement fields for bolt pattern #5; Displacements in mm × 10^{-3} (0.03937 in × 10^{-3}); A–C: perpendicular to load; D–F: parallel to load; A. & D. load = 8.896 kN (2,000 lb), B. & E. load = 35.58 kN (8,000 lb), C. & F. load = 53.38 kN (12,000 lb).

increases, the surface displacements perpendicular to load beneath the bolts split along the centerline of the bolts even at relatively low load levels due to the Poisson effect and low tension perpendicular to the grain properties of wood, where the left half of the connection moves left and the right half of the connection moves right. Because wood members often split parallel to a vertical row of connectors in practice, the trends in the displacements fields observed in this study could be used to predict the onset and location of potentially catastrophic joint failures. The displacement fields could also be used to study the influence of bolt spacing and the number of bolts.

- For three bolts in a horizontal column, the parallel to load displacements below the bolt nearest the load were greater than those beneath the other bolts and not equal to the last bolt in the series as previously reported (Cramer 1968 and Lantos 1969). It is suggested that this conflict should lead to further study.
- For multi-bolt patterns in a horizontal column, there did not appear to be any development of a well-defined trend in the surface displacements as the number of bolts increased. The perpendicular displacements may or may not be concentrated on one side of the connection, which indicates less of a tendency of the wood side members to split perpendicular to the grain as the number of bolts increases in a horizontal column.
- The digital image correlation method is an effective qualitative and quantitative technique for describing surface displacement fields, both parallel and perpendicular to load, beneath the bolts of single- and multiple-bolted wood connections. Variation in material properties, rigid body motion, eccentric loading, and/or wood failure beneath a bolt are detectable with DICT, and unless these factors are not carefully considered, they may influence the results obtained with digital image correlation when applied to wood test specimens.

ACKNOWLEDGMENTS

The authors wish to acknowledge support for this project by USDA NRI Grant #93-1244-01 and assistance with the correlation analysis by Dr. Michael A. Sutton, Mechanical Engineering, University of South Carolina, Columbia, SC.

REFERENCES

AGRAWAL, C. P. 1989. Full-field deformation measurement in wood using digital image processing. M.S. thesis, Dept. of Wood Science and Forest Products, Virginia Tech, Blacksburg, VA. 103 pp.

AMERICAN FOREST AND PAPER ASSOCIATION (AFPA). 1993. ANSI/NFoPA NDS. 1991. National design specification for wood construction. AFPA, Washington, DC. 125 pp.

AMERICAN SOCIETY FOR TESTING AND MATERIALS (ASTM). 1993. Standard test methods for mechanical fasteners in wood. ASTM D 1761. Annual Book of Standards, sect. 4, vol. 4.09. 1993. Philadelphia, PA.

CHOI, D., J. L. THORPE, AND R. B. HANNA. 1991. Image analysis to measure strain in wood and paper. Wood Sci. Technol. 25:251–262.

CHU, T. C., W. F. RANSON, AND M. A. SUTTON. 1985. Applications of digital-image-correlation techniques to experimental mechanics. Exp. Mech. 25(3):232–245.

CRAMER, C. O. 1968. Load distribution in multiple-bolt tension joints. J. Struct. Div. ASCE, vol. 94, no. ST5, May.

FANTOZZI, J., AND P. E. HUMPHREY. 1995. Effects of bending moments on the tensile performance of multiple-bolted timber connectors. Part I: A technique to model such joints. Wood Fiber Sci: 27(1):55–67.

HE, Z. H., M. A. SUTTON, W. R. RANSON, AND W. H. PETERS. 1984. 2-D fluid velocity measurements by use of digital speckle correlation techniques. Exp. Mech. 24(2):117–121.

HUMPHREY, P. E. AND L. J. OSTMAN. 1989a. Bolted timber connections. Part I: A wafer technique to model wood deformation around bolts. Wood Fiber Sci: 21(3):239–251.

———, AND———. 1989b. Bolted timber connections. Part II. Bolt bending and associated wood deformation. Wood Fiber Sci: 21(4):354–366.

JORISSEN, A. 1996. Multiple fastener timber connections with dowel type fasteners. International Wood Engineering Conference, New Orleans, LA. 4:189–196.

KERMANI, A., AND W. M. C. MCKENZIE. 1994. The use of single-beam reflection holography to determine strain distributions around bolts. J. Inst. Wood Sci. 13(4):454–458.

LANTOS, G. 1969. Load distribution in a row of fasteners subjected to lateral load. Wood Sci. 1(3):129–136.

LUO, P. M., Y. J. CHAO, AND M. A. SUTTON. 1994. Experimental evaluation of J-integral using both in-plane

deformations and caustics obtained from out-of-plane displacements. Pages 248–253 in Proc. 1994 Spring Conference on Experimental Mechanics, Baltimore, MD.

PETERS, W. H., AND W. F. RANSON. 1982. Digital imaging techniques in experimental stress analysis. Opt. Eng. May/June 21(3):427–431.

———, ———, M. A. SUTTON, T. C. CHU, AND J. ANDERSON. 1983. Application of digital correlation methods to rigid body mechanics. Opt. Eng. Nov./Dec. 22(6):738–742.

RAHMAN, M. U., Y. J. CHIANG, AND R. E. ROWLANDS. 1991. Stress and failure analysis of double-bolted joints in Douglas-fir and Sitka spruce. Wood Fiber Sci. 23(4): 567–589.

RANSON, W. F., D. M. WALKER, AND J. B. CAULFIELD. 1986. Biomechanics. *in* Computer vision in engineering mechanics. A discussion paper prepared for the NSF workshop on solid mechanics related to paper. August, 1986, Blue Mountain Lake, NY.

ROWLANDS, R. E., M. U. RAHMAN, T. L. WILKINSON, AND Y. I. CHIANG. 1982. Single- and multiple-bolted joints in orthotropic materials. Composites 13(3):273–279.

SALINEKOVICH, A., J. R. LOFERSKI, AND A. G. ZINK. 1996. Understanding the performance of laterally loaded wood connections assembled with multiple bolts. Wood Design Focus 7(4):19–26. Forest Products Society, Madison, WI.

STELMOKAS, J. W. 1995. Two novel techniques to study multiple-bolted wood connection behavior. M.S. thesis, Virginia Tech, Blacksburg, VA.

———, A. G. ZINK, J. R. LOFERSKI, AND J. D. DOLAN. 1997. Measurement of load distribution among multiple-bolted wood connections. ASTM J. Testing Eval. In press.

SUTTON, M. A. AND Y. J. CHAO. 1988. Measurement of strains in a paper tensile specimen using computer vision and digital image correlation. Part I: Data acquisition and image analysis system. Tappi 71(3):173–175.

VENDROUX. G. 1994. Scanning tunneling microscopy in micromechanics investigations. Ph.D thesis, California Inst. of Technology, Pasadena, CA

WILKINSON, T. L. 1986. Load distribution among bolts to load. J. Struct. Eng. 112(4):835–852.

———, AND R. E. ROWLANDS. 1981. Analysis of mechanical joints in wood. Exp. Mech. 21(11):408–414.

ZINK, A. G. 1992. The influence of overlap length on the stress distribution and strength of a bonded wood double lap joint. Ph.D. dissertation, State University of New York, Syracuse,. NY.

———. R. W. DAVIDSON, AND R. B. HANNA. 1995. Strain measurement in wood using a digital image correlation technique. Wood Fiber Sci. 27(4):349–359.